THE JOURNAL OF PHYSICAL CHEMISTRY B

Article

pubs.acs.org/JPCB

Solid-State NMR Analyses Reveal the Structure Dependence of the Molecular Dynamics for ω-Amino Acids

Jing Huang,[†,‡] Limin Zhang,[†] and Huiru Tang*[,†]

[†]State Key Laboratory of Magnetic Resonance and Atomic and Molecular Physics, Wuhan Centre for Magnetic Resonance, Wuhan Institute of Physics and Mathematics, Wuhan 430071, P.R. China

[‡]Graduate University of Chinese Academy of Sciences, Beijing 100049, P.R. China

Supporting Information

ABSTRACT: The molecular dynamics of metabolites is structure dependent and vitally important for the interactive functions in their potential applications as natural materials. To understand the relationship between molecular structure and dynamics, the molecular motions of four structurally related ω-amino acids (β-alanine, γ-aminobutyric acid, 5-aminovaleric acid, and 6-aminocaproic acid) were investigated by measuring their proton spin−lattice relaxation times (T_1, $T_{1\rho}$) as a function of temperature (180−440 K). ^{13}C CPMAS NMR and DSC analyses were performed to obtain complementary information. All of these ω-amino acids showed no phase transition in the temperature range studied but had outstandingly long proton T_1 at 300 MHz and even at 20 MHz for the deuterated forms. The molecular dynamics of all these ω-amino acids were dominated by the reorientation motions of amino groups and backbone motions except in β-alanine. The activation energies for amino group reorientations were positively correlated with the strength of hydrogen bonds involving these groups in the crystals and the carbon-chain lengths, whereas such energies for the backbone motions were inversely correlated with the carbon-chain lengths. These findings provided essential information for the molecular dynamics of ω-amino acids and demonstrated the combined solid-state NMR methods as a useful approach for understanding the structural dependence of molecular dynamics.

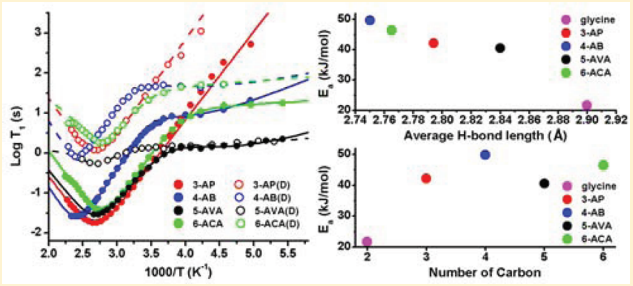

1. INTRODUCTION

The structure−property relationships are of great importance for both fundamental and applied research especially when the metabolite bioactivities, functions of polymers, and properties of pharmaceuticals are considered. This notion is highlighted by the structure−activity relationships (SAR) for plant secondary metabolites in terms of their interactions with biopolymers[1] and their neuroprotective functions.[2] It is also known that the polymorphic properties are closely related to the molecular dynamics[3,4] for the aliphatic α-amino acids with linear side-chains[5,6] and drugs underpinning their physical, pharmacological, and stability properties. In fact, structural dependence of molecular dynamics is present, as our previous study has already shown for the methylation effects on the molecular motions of N-methylated glycines,[7] where the motional properties for different methyl groups differ significantly.

A series of simple molecules with a distribution of structural properties is often required as a useful model system to understand the aforementioned structure−dynamics relationships. For this purpose, ω-amino acids including glycine, 3-aminopropanoic acid (3-AP), 4-aminobutyric acid (4-AB), 5-aminovaleric acid (5-AVA), and 6-aminocaproic acid (6-ACA) represent a set of such molecules, since they have a nice distribution of carbon-chain lengths and intermolecular interactions in their crystals.

Information for the molecular dynamics of these ω-amino acids offers some extra values, since they are either biologically active molecules or have important industrial applications. Among them, 3-AP is a nonproteogenic amino acid and formed by proteolytic degradation of β-alanine-containing dipeptides such as carnosine, anserine, and pantothenic acid (vitamin B_5).[8] This metabolite can also be synthesized via the catabolism of pyrimidine-based nucleotides in liver through uracil and dihydrouracil. Under normal conditions, 3-AP is metabolized to aspartic acid with glutamic acid decarboxylase (GAD) or converted into malonate semialdehyde entering propanoate metabolism. As a rate-limiting precursor of carnosine,[9] supplementation with 3-AP increases carnosine concentration in muscles and decreases fatigue in athletes.[10,11] In contrast, 4-AB is an inhibitory neurotransmitter in the vertebrate central nervous system[12] and synthesized from glutamate catalyzed by GAD. 4-AB can be eliminated by entering the Krebs cycle via succinic acid catalyzed with GABA-transaminase and succinic semialdehyde dehydrogenase.[13] 5-AVA is a normal metabolite present in human saliva and elevated in patients with chronic periodontitis.[14] 6-ACA is used as an effective treatment for

Received: December 2, 2011
Revised: January 17, 2012
Published: January 17, 2012

excessive postoperative bleeding, especially fibrogenemia, since it is an effective inhibitor for enzymes (such as plasmin) responsible for fibrinolysis.[15] 5-AVA and 6-ACA are also well-known as intermediates for nylon-5 and nylon-6, respectively, and for synthesis of biodegradable copolymers.[16,17]

The crystal structures of these four ω-amino acids have all been reported. 3-AP had crystals in the orthorhombic with space group *P*bca and had eight molecules in one unit cell.[18] These 3-AP molecules were present as zwitterions in its crystals where each amino group formed three hydrogen bonds with the carbonyl groups having similar H-bond lengths of 2.795, 2.753, and 2.833 Å, respectively.[18] 4-AB crystallized in the monoclinic with space group $P2_1/a$ and had four molecules in one unit cell.[19] The molecular geometry of 4-AB was not a planar trans-zigzag configuration but a gauche configuration with respect to the $C_\alpha-C_\beta$ bond. 4-AB molecules were also present as zwitterions in its crystals where each molecule involved in three N−H···O hydrogen bonds with bond lengths of about 2.733−2767 Å.[19] The synchrotron powder diffraction data for 5-AVA[20] showed that there were four molecules in its unit cell and each molecule possessed approximately a mirror symmetry perpendicular to the *c*-axis; two oxygen atoms did not locate at the positions with the symmetry to each other. There were three short intermolecular N−H···O contacts in its crystal structure with hydrogen-bond lengths of 2.77−2.89 Å.[20] 6-ACA had crystals in the monoclinic with space group $P2_1/c$ and four molecules in its unit cell.[21] These molecules were present as zwitterions in the crystals, and each molecule participated in three intermolecular hydrogen bonds (N−H···O) with adjacent molecules, forming a double-layered structure.[21] These hydrogen-bond lengths were about 2.728, 2.753, and 2.814 Å, respectively.[21] Since the amino groups in the above four amino acid crystals all form (three) intermolecular hydrogen bonds, their motions are expected to be affected by the properties of these hydrogen-bond systems, although the nature of such effects remains to be elucidated.

The combination of various solid-state NMR techniques is well-established as being effective for probing molecular dynamics in multiple time scales. The proton NMR relaxation measurements are powerful for studying molecular motions in the time scale of nano- to microseconds, while measurements of dipolar interactions, chemical shift anisotropy, and exchanges offer dynamics information in the time range of microseconds to a few seconds. In fact, such combined solid-state NMR methods have already been successfully employed in a number of studies of molecular dynamics including amino acid derivatives[22,23] and plant cell-wall related monosaccharides.[24,25] These methods have also been used for understanding the molecular structure, dynamics, and interactions in more complex systems such as carbohydrate glasses,[26,27] polymers,[28−30] and heterogeneous plant polysaccharides[31−33] over a range of motional frequencies.

In this paper, we investigated the molecular dynamics of 3-AP, 4-AB, 5-AVA, 6-ACA, and their deuterated forms by measuring proton relaxation times in the laboratory and rotating frames. Complementary information was also obtained with high resolution ^{13}C CPMAS NMR spectroscopy and differential scanning calorimetry. The objectives of this study are (1) to obtain motional information for these amino acids and (2) to explore potential structure dependence of the molecular dynamics properties for this set of molecules.

2. EXPERIMENTAL SECTION

2.1. Materials. 3-Aminopropanoic acid (3-AP), 4-aminobutyric acid (4-AB), 5-aminovaleric acid (5-AVA), and 6-aminocaproic acid (6-ACA) were all purchased from Sigma-Aldrich with quoted purities as 99 or 98% and used without further purification. Their melting points were 202, 203, 157.5, and 205 °C, respectively, according to Sigma data. Figure 1

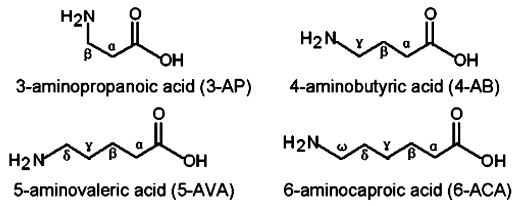

Figure 1. Molecular structures for the ω-amino acids studied.

shows schematic forms of their molecular structures. They were all dried over P_2O_5 in a desiccator under vacuum for at least 1 week prior to experiments, and these samples were referred to the protonated samples. The protonated samples were respectively dissolved in pure D_2O (about 300 mg of each sample in 1.5 mL of D_2O) and lyophilized. The process was repeated three times, and the obtained samples were referred to the deuterated samples. These samples were further dried over P_2O_5 in a desiccator under vacuum for at least 3 days prior to analysis.

2.2. Differential Scanning Calorimetry (DSC) Studies. DSC analyses of protonated 3-AP, 4-AB, 5-AVA, and 6-ACA were performed on a Pekin-Elmer Pyris 1 Calorimeter in a sealed aluminum pan for each sample (about 5 mg). The temperature range was chosen between 123 K and the sample's melting point. The measurements were carried out using boiling-off liquid nitrogen as the cooling gas and helium as the purge gas with a heating and cooling rate of 10 K/min. All samples were first cooled to 123 K from room temperature and subsequently heated to the samples' melting points followed by cooling to 123 K. The heat flow was recorded as a function of temperature.

2.3. High Resolution ^{13}C CPMAS Spectroscopy. The high resolution ^{13}C CPMAS experiments were carried out on a Varian Infinity Plus 300 spectrometer operating at 299.75 and 75.38 MHz for ^1H and ^{13}C, respectively. The 90° pulse-length was 2.98 μs for ^1H, and the Hartmann−Hahn matching condition was set up with each sample. The cross-polarization contact time varied from 0.4 to 0.5 ms to obtain the best signal-to-noise ratio. The acquisition time was limited to 60 ms with a proton-decoupling field strength of about 60 kHz to avoid stresses to hardware. The ^{13}C chemical shifts were referenced to a solid hexamethylbenzene sample externally (17.35 ppm for the methyl group). The ^{13}C CPMAS spectra of 3-AP, 5-AVA, and 6-ACA were obtained at room temperature; the spectrum of 4-AB was obtained at 343 K, since we could not get a signal in its ^{13}C CPMAS spectrum at room temperature due to its extremely short proton $T_{1\rho}$ at room temperature as in the case of glycine.[34] Due to the exceedingly long ^1H T_1 (>30 s), more complex ^{13}C CPMAS experiments such as DIPSHIFT and ^{13}C T_1 measurements were not practical.

2.4. Proton Relaxation Time Measurements. The proton spin−lattice relaxation time in the laboratory frame, T_1, and in the rotating frame, $T_{1\rho}$, together with the proton second moment, M_{2r}, were measured on a Bruker Mq-20

dx.doi.org/10.1021/jp211623n | J. Phys. Chem. B 2012, 116, 2096−2103

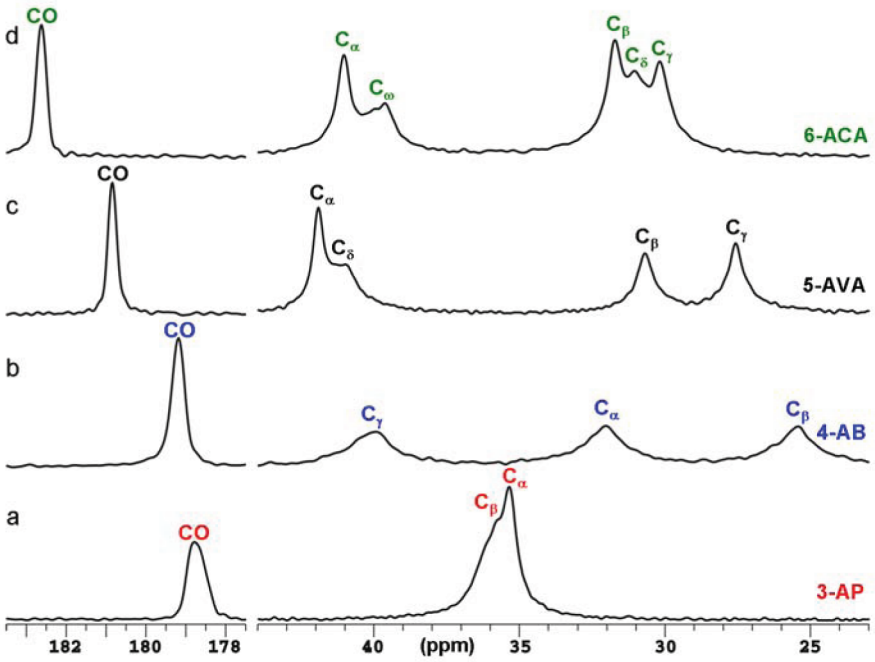

Figure 2. ^{13}C CPMAS NMR spectra for 3-aminopropanoic acid (3-AP), 4-aminobutyric acid (4-AB), 5-aminovaleric acid (5-AVA), and 6-aminocaproic acid (6-ACA).

Table 1. ^{13}C Chemical Shifts for Carbons in 3-Aminopropanoic Acid (3-AP), 4-Aminobutyric Acid (4-AB), 5-Aminovaleric Acid (5-AVA), and 6-Aminocaproic Acid (6-ACA) in the Solid State

compounds	CO	C_α	C_β	C_γ	C_δ	C_ω
3-AP	178.6	35.4	36.2/35.8			
4-AB	179.2	32.1	25.5	40.0		
5-AVA	180.8	41.9	30.7	27.6	41.3/41.0	
6-ACA	182.6	41.0	31.7	30.2	31.1	40.0/39.6

spectrometer (19.95 MHz) with a proton 90° pulse-length of 2.85 μs. T_1 was measured using the saturation-recovery pulse sequence (recycle delay-90°-τ-90°-acquisition) with 20 relaxation delays except for the very long T_1 where 16 relaxation delays were used. The spread of relaxation delays was selected to cover the length equivalent to about $5T_1$; the relaxation processes for all of these compounds were found to be monoexponential within experimental error in the whole temperature range. $T_{1\rho}$ was measured using the standard sequence (recycle delay-90°-spin lock-acquisition)[35] with a spin-lock field of about 45 kHz. Sixteen spin-lock delays varying from 0.04 to 300 ms were used. The decays of nuclear magnetization were found to be monoexponential within experimental error in the whole temperature range.

M_{2r} was measured using the solid-echo pulse sequence [recycle delay-90°$_x$-τ_1-90°$_y$-τ-acquisition][36] to obtain the complete Bloch decay.[37] τ_1 was 13 μs, and τ was chosen to be (11 μs) slightly longer than the dead-time of the spectrometer to ensure observation of an echo. The decay parts of the solid echoes were fitted to a modified Gaussian function to obtain the M_{2r} values.[38,39]

Sample temperature was controlled with a Bruker variable-temperature unit, VT-3000, with a temperature range of 178–460 K. Temperatures below room temperature were controlled with gas from liquid-nitrogen, and all variable-temperature experiments were started from the lowest temperature with an increment of 10 K. A total of 15 min waiting time was allowed to ensure temperature stabilization and equilibration with temperatures stabilized within ±1 K. The actual sample temperatures were calibrated by directly inserting a precalibrated thermal couple into a sample-filled tube in the probe head. All relaxation time values were extracted by curve-fitting using a Ladenburg–Marquardt nonlinear curve-fitting routine.

3. RESULTS AND DISCUSSION

3.1. Differential Scanning Calorimetry (DSC). The DSC curves of protonated 3-AP, 4-AB, 5-AVA, and 6-ACA showed no endothermic or exothermic process except the melting processes over the temperature range between 123 K and the sample's melting point (data not shown). This indicated that there were no solid–solid phase transitions for these four compounds in the temperature range studied.

3.2. ^{13}C CPMAS NMR Spectroscopy. Figure 2 shows ^{13}C CPMAS NMR spectra for 3-AP, 4-AB, 5-AVA, and 6-ACA with their resonances assigned (Table 1). For 3-AP, two peaks at 36.2 and 35.8 ppm (Figure 2a) were assigned to the C_β (CH_2) and such peak splitting (about 30 Hz) was due to $^{13}C-^{14}N$ coupling.[40,41] This is further confirmed with the detection of only one single resonance (35.8 ppm) for this moiety (Figure S1, Supporting Information) at a higher magnetic field (9.4 T, ^{13}C 100.6 MHz), since residual $^{13}C-^{14}N$ dipolar coupling decreases with the increase of magnetic field.[42] Resonances at 35.4 and 178.8 ppm (Figure 2a) were readily assignable to α-CH_2 and carbonyl moieties.

dx.doi.org/10.1021/jp211623n | J. Phys. Chem. B 2012, 116, 2096–2103

For 4-AB, four resonances were observed at 179.2, 40.0, 32.1, and 25.5 ppm (Figure 2b) corresponding to carbonyl and three methylene moieties, respectively. The signal at 40.0 ppm was assigned to γ-CH_2, since the quadrupolar effects of ^{14}N resulted in a much broader line-shape compared with the other two methylene signals. The signals at 32.1 and 25.5 ppm were tentatively assigned to α-CH_2 and β-CH_2, respectively, according to their chemical shifts in aqueous solution. For 5-AVA, the signal with two resonance lines at 41.3 and 41.0 ppm (Figure 2c, Figure S2, Supporting Information) were assigned to the nitrogen-bearing carbon (δ-CH_2) with about 22 Hz splitting from $^{13}C-^{14}N$ coupling[40,41] as in the case of 3-AP. The resonance at 180.8 ppm (Figure 2c) was readily assigned to the CO moiety, and the one at 41.9 ppm (Figure 2c) was assigned to α-CH_2, since this carbon is attached to a carbonyl group and should appear at lower field than β-CH_2 and γ-CH_2 (at 30.7 and 27.6 ppm). In the case of 6-ACA, the signals at 40.0 and 39.6 ppm (Figure 2d, Figure S2, Supporting Information) were assigned to the nitrogen-bearing ω-CH_2 with a $^{13}C-^{14}N$ coupling of 30 Hz,[40,41] whereas the signal at 41.0 ppm was assigned to α-CH_2 as above. The signals at 31.7, 31.1, and 30.2 ppm (Figure 2d) were tentatively assigned to δ-CH_2, β-CH_2, and γ-CH_2, respectively, while a signal at 182.6 ppm was readily assignable to the carbonyl moiety.

3.3. Proton Spin−Lattice Relaxation in the Laboratory Frame. At 300 MHz, ^1H T_1 measured through ^{13}C CPMAS spectra for 3-AP and 6-ACA was exceedingly long (about 58.6 and 30.4 s, respectively) at ambient temperature (Figure S3, Supporting Information); ^1H T_1 was not measurable for 4-AB at ambient temperature due to its extremely short ^1H $T_{1\rho}$, but it was also extremely long (33.2 s) at 343 K (Figure S3, Supporting Information). ^1H T_1 for 5-AVA (about 5 s) was much shorter at the similar temperature (Figure S3, Supporting Information). This makes it impractical to perform more complex experiments relying on the ^{13}C CPMAS spectra such as temperature dependence of ^{13}C T_1 and DIPSHIFT. At 20 MHz, in contrast, ^1H T_1 values at the ambient were about 0.23, 2.67, 0.31, and 0.46 s for the protonated 3-AP, 4-AB, 5-AVA, and 6-ACA, respectively. Such values were much greater (11.6, 42, 1.3, and 11.3 s, respectively) for the deuterated 3-AP, 4-AB, 5-AVA, and 6-ACA. This implies that amino groups in these amino acids are important relaxation contributors at room temperature. Therefore, only relaxation data from the 20 MHz spectrometer were further analyzed in detail.

The proton spin−lattice relaxation rates in the laboratory frame (at 20 MHz), R_1, were plotted as a function of temperature (Figure 3) for 3-AP, 4-AB, 5-AVA, and 6-ACA. An R_1 maximum at about 350−420 K was observable for all these compounds and readily assignable to the 3-fold rotations of amino groups, since these maxima were almost completely diminished upon D_2O exchange. Another weak relaxation process was observable for 4-AB, 5-AVA, and 6-ACA at lower temperature (e.g, about 219 K for 5AVA). Upon deuteration, this low temperature process did not change much, indicating that this process involved nonexchangeable protons.

To evaluate these motions quantitatively, the experimental data were fitted to the well-known Kubo−Tomita expression[43−45] assuming exponential correlation functions

$$R_1 = \frac{1}{T_1} = \sum_{i\geq 1} C_i \left[\frac{\tau_{ci}}{1+\omega_0{}^2\tau_{ci}{}^2} + \frac{4\tau_{ci}}{1+4\omega_0{}^2\tau_{ci}{}^2} \right] \quad (1)$$

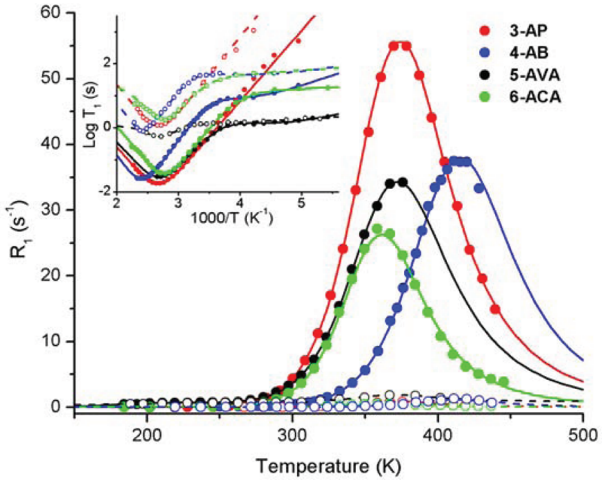

Figure 3. Proton spin−lattice relaxation rates in the laboratory frame as a function of temperature for 3-aminopropanoic acid (3-AP), 4-aminobutyric acid (4-AB), 5-aminovaleric acid (5-AVA), and 6-aminocaproic acid (6-ACA). The inset is a plot of log T_1 versus 1000/T for these compounds. The filled and empty symbols are data from the protonated and deuterated samples, respectively. The solid and dashed lines are corresponding fitted data.

where ω_0 is the proton Larmor frequency and τ_{ci} is the rotational correlation time of the motions responsible for the spin−lattice relaxation, which is assumed to follow the Arrhenius activation law:

$$\tau_{ci} = \tau_{0i} \exp\left(\frac{E_{ai}}{RT}\right) \quad (2)$$

where τ_{0i} is the pre-exponential factor corresponding to the motional correlation time at infinite temperature, E_{ai} is the activation energy, and R the gas constant. C_i is the relaxation constant which is given by eq 3 for amino groups assuming that the motion occurring is fast on the NMR relaxation time scale:

$$C_i = \frac{9}{20}\frac{n_i}{N_i}\frac{\gamma^4\hbar^2}{r^6} \quad (3)$$

where γ is the proton magnetogyric ratio, N_i is the total number of protons in their molecules, n_i is the number of protons contributing to the relaxation process, and r is the average interproton distance in amino groups.

When we used a model with single thermally activated motion to fit the experimental data, obvious discrepancies were observable between the theoretical and experimental data at low temperature for all of these amino acids except 3-AP; such discrepancies were much more pronounced for 5-AVA. In contrast, when a model with two thermally activated processes was employed for 4-AB, 5-AVA, and 6-ACA, the theoretical and experimental data agreed reasonably well (Figure 3). Similar observations have already been made for insulin[46] and DL-methionine.[47] This indicates that, at low temperatures when the relaxation of amino group rotation is no longer efficient, other weaker motional processes become evidently observable including carbon-chain motions involving CH_2 moieties.[46] Such a notion is further confirmed by the fact that the relaxation processes at low temperatures are still present (inset in Figure 3) for the deuterated 4-AB, 5-AVA, and 6-ACA. Therefore, two thermally activated motions were considered to analyze the experimental data of 4-AB, 5-AVA, and 6-ACA as

dx.doi.org/10.1021/jp211623n | J. Phys. Chem. B 2012, 116, 2096−2103

Table 2. Relaxation Parameters for 3-Aminopropanoic Acid (3-AP), 4-Aminobutyric Acid (4-AB), 5-Aminovaleric Acid (5-AVA), and 6-Aminocaproic Acid (6-ACA)

	activation energy E_a (kJ/mol)	pre-exponential factor τ_0 (10^{-14} s)	relaxation constant C (10^9 rad s^{-2})	T_1^{min} or $T_{1\rho}^{min}$ [a] (ms)	temperature at T^{min} [b] (K)
3-AP (H)					
NH_3^+ (T_1)[c]	42.2 ± 0.0	0.62 ± 0.03	4.87 ± 0.01	18.1	373
NH_3^+ ($T_{1\rho}$)[d]	25.6 ± 1.0	650 ± 290	4.40 ± 0.13	0.3	259
3-AP (D)[e]					
NH_3^+ (T_1)	45.3 ± 0.8	0.22 ± 0.05	0.074 ± 0.001	1190.5	373
4-AB (H)					
backbone (T_1)	12.7 ± 0.6	(1.21 ± 0.42) × 10^3	0.010 ± 0.0002	9174.3	268
NH_3^+ (T_1)	49.7 ± 0.4	0.27 ± 0.04	3.34 ± 0.05	26.4	414
NH_3^+ ($T_{1\rho}$)	30.5 ± 0.8	367 ± 113	3.08 ± 0.05	0.4	293
4-AB (D)[e]					
backbone (T_1)	7.3 ± 3.1	(1.33 ± 1.93) × 10^4	0.0019 ± 0.0001	46511.6	242
NH_3^+ (T_1)	53.9 ± 1.8	0.07 ± 0.04	0.098 ± 0.003	900.9	410
NH_3^+ ($T_{1\rho}$)	39.6 ± 2.1	7.5 ± 6.3	0.173 ± 0.006	7.3	289
5-AVA (H)					
backbone (T_1)	9.6 ± 0.7	(2.87 ± 1.12) × 10^3	0.061 ± 0.001	1446.1	223
NH_3^+ (T_1)	40.5 ± 0.8	1.02 ± 0.30	3.01 ± 0.07	29.3	373
NH_3^+ ($T_{1\rho}$)	25.3 ± 0.5	652 ± 158	2.29 ± 0.04	0.6	256
5-AVA (D)[e]					
backbone (T_1)	2.6 ± 1.7	(3.22 ± 5.85) × 10^5	0.077 ± 0.044		
NH_3^+ (T_1)	48.0 ± 6.8	0.08 ± 0.19	0.093 ± 0.011	947.9	369
NH_3^+ ($T_{1\rho}$)	32.9 ± 1.3	15.7 ± 10.0	0.135 ± 0.003	9.3	253
6-ACA (H)					
backbone (T_1)	2.1 ± 4.9	7.02 × 10^6 ± 5.74 × 10^9	0.012 ± 97		
NH_3^+ (T_1)	46.4 ± 0.8	0.10 ± 0.02	2.31 ± 0.05	38.2	362
NH_3^+ ($T_{1\rho}$)	27.8 ± 0.9	266 ± 105	1.75 ± 0.04	0.7	259
6-ACA (D)[e]					
backbone (T_1)	2.6 ± 4.8	2.49 × 10^6 ± 2.54 × 10^8	0.015 ± 1.47		
NH_3^+ (T_1)	47.2 ± 2.3	0.08 ± 0.06	0.045 ± 0.002	1964.6	362
glycine					
NH_3^+	21.7[f]		6.29[g]		325[f]

[a]Relaxation time values at their minima. [b]Temperature at the minimum relaxation time. [c]Results from T_1 data. [d]Results from $T_{1\rho}$ data. [e]Data from the deuterated samples. [f]Data taken from ref 58. [g]Data taken from ref 49.

well as their deuterated forms. 3-AP failed to show such carbon-chain motions probably due to its restricted carbon numbers in the light of hydrogen-bonding systems formed by amino and carboxyl groups.

The results in Figure 3 indicated that the experimental data for all of these amino acids agreed reasonably well with the theoretical ones. The motional relaxation parameters obtained from the curve-fitting are tabulated in Table 2. The 3-fold rotation of the amino group in 3-AP had an E_a value of 42.2 kJ/mol and τ_0 value of 6.2 × 10^{-15} s, being in good agreement with the reported values for similar amino groups.[5,22,47−50] The relaxation constant C value was 4.87 × 10^9 rad s^{-2}. Assuming the protons in the amino group were equilateral and the major contributors to the C value, the calculated average interproton distance was 1.681 (±0.001) Å according to eq 3. The corresponding N−H bond-length was thus 1.029 (±0.001) Å assuming the nitrogen atom in the amino group adopted a perfect tetrahedral geometry. This value of N−H bond length is slightly larger than the values of 0.951, 0.958, and 0.927 Å from its X-ray structure data.[18] However, our data agreed well with the results for L-alanine,[51] L-valine hydrochloride,[52] glycine hydrochloride,[53] and L-tyrosine[54] obtained from neutron scattering data. This is not surprising, since proton positions in X-ray data are often not reliable. The relaxation constant of amino group rotation for the deuterated sample (7.4 × 10^7 rad s^{-2}) was only a fraction of that for the protonated sample, indicating almost complete deuterium exchanges for amino group protons.

The E_a and τ_0 values for the 3-fold rotation of the amino group in 4-AB were 49.7 kJ/mol and 2.7 × 10^{-15} s, respectively, which agreed with the reported values for similar amino groups.[5,22,47−50] On the basis of the relaxation constant (3.34 × 10^9 rad s^{-2}), the calculated average interproton distance (1.717 ± 0.004 Å) and N−H bond length (1.051 ± 0.003 Å) were consistent with those values for the commonly encountered amino groups.[51−54] The relaxation constant C for the deuterated 4-AB (9.8 × 10^7 rad s^{-2}) was only a fraction of that for the protonated sample, indicating almost complete exchange for protons in the amino group. The low temperature relaxation process had an E_a value of 12.7 kJ/mol and τ_0 value of 1.21 × 10^{-11} s.

For 5-AVA, the 3-fold rotation of the amino group had an E_a value of 40.5 kJ/mol and τ_0 value of 1.02 × 10^{-14} s, being in good agreement with the literature values for similar groups.[5,22,47−50] On the basis of the relaxation constant C (3.01 × 10^9 rad s^{-2}) for amino group rotation, the calculated average interproton distance (1.689 ± 0.007 Å) and the corresponding N−H bond length (1.034 ± 0.004 Å) were all in accord with that for the amino groups in 3-AP, 4-AB, and the other commonly encountered amino acids.[51−54] The C value

dx.doi.org/10.1021/jp211623n | J. Phys. Chem. B 2012, 116, 2096−2103

for the amino group of the deuterated 5-AVA (9.3×10^7 rad s^{-2}) was only a fraction of that for the protonated sample, suggesting almost complete deuteration. A low temperature relaxation process had an E_a value of 9.6 kJ/mol and τ_0 value of 2.87×10^{-11} s. The low temperature motional process had a slightly larger C value (7.7×10^7 rad s^{-2}) than that for the protonated sample (6.1×10^7 rad s^{-2}). This indicated that the low temperature process was probably due to limited motions of nonexchangeable protons (i.e., backbone CH_2 moieties). 6-ACA had an E_a value of 46.4 kJ/mol and τ_0 value of 1.0×10^{-15} s for the 3-fold rotation of the amino group, which agreed well with the reported values for similar groups.[5,22,47−50] From the relaxation constant C value (2.31×10^9 rad s^{-2}), the calculated average interproton distance for the amino group (1.717 ± 0.006 Å) and the corresponding N−H length (1.051 ± 0.004 Å) were in accord with those for 3-AP, 4-AB, 5-AVA, and common amino acids.[51−54]

The low temperature relaxation process for 4-AB, 5-AVA, and 6-ACA had an E_a value of 2−13 kJ/mol corresponding to motions of the carbon chains, since deuteration did not eliminate such a relaxation sink (inset in Figure 3). C values ($2-70 \times 10^6$ rad s^{-2}) for this motion were much smaller than those for the rotational motions of amino groups, probably indicating the restricted magnitude for such motions of CH_2 moieties. With limited data points, τ_0 values for this process had large fitting errors and thus were not discussed.

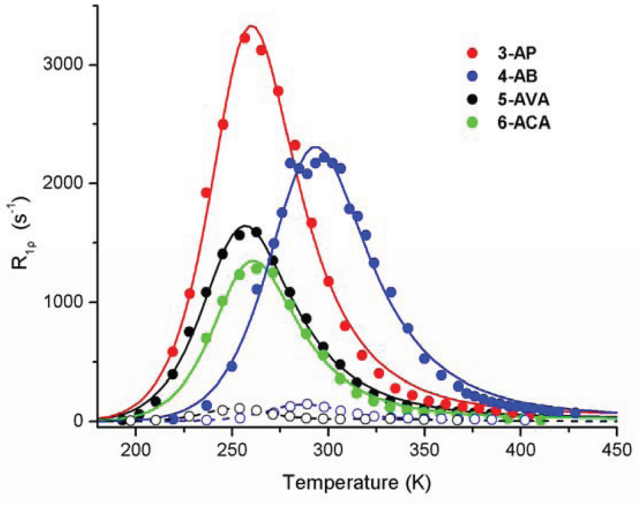

Figure 4. Proton spin−lattice relaxation rates in the rotating frame as a function of temperature for 3-aminopropanoic acid (3-AP), 4-aminobutyric acid (4-AB), 5-aminovaleric acid (5-AVA), and 6-aminocaproic acid (6-ACA). The filled and empty symbols are data from the protonated and deuterated samples, respectively. The solid and dashed lines are fitted data.

3.4. Proton Spin−Lattice Relaxation in the Rotating Frame. The proton spin−lattice relaxation rates in the rotating frame, $R_{1\rho}$, are plotted in Figure 4 as a function of temperatures for both of the protonated and some deuterated samples. There was only one maximum of $R_{1\rho}$ at 259, 293, 256, and 259 K for 3-AP, 4-AB, 5-AVA, and 6-ACA, respectively. These maxima were all attributed to the rotations of amino groups with the maxima in 4-AB and 5-AVA diminished upon deuteration.

The $R_{1\rho}$ data were fitted to an expression similar to that used in R_1 analysis:[25,45]

$$R_{1\rho} = \frac{1}{T_{1\rho}} = \frac{3}{2}\sum_{i\geq 1} C_i\left[\frac{\tau_{ci}}{1+4\omega_{ei}^2\tau_{ci}^2} + \frac{5}{3}\times\frac{\tau_{ci}}{1+4\omega_0^2\tau_{ci}^2} + \frac{2}{3}\times\frac{\tau_{ci}}{1+4\omega_0^2\tau_{ci}^2}\right] \quad (4)$$

where ω_0, τ_{ci}, and C_i have the same meaning as in the previous expressions and ω_{ei} is the effective field for relaxation in frequency unit. Since the spin-lock field (ω_{SP}, about 45 kHz) and the local dipolar field strength (ω_L, about 50 kHz) were similar in this study, these two terms were taken into consideration using the McCall−Douglass equation[55] (eq 5):

$$\omega_e = \sqrt{\omega_{SP}^2 + \omega_L^2} \quad (5)$$

In practice, ω_L is temperature dependent, and the temperature dependence of ω_L for the above four molecules can be modeled satisfactorily by fitting the second moment data to a sigmoid function to give the closest values to the experimental ones, within the temperature range studied.

The experimental data agreed well with the calculated ones with the above equations (Figure 4), and the relaxation parameters obtained from the curve-fitting were tabulated in Table 2. These results indicated that the relaxation constants for amino groups obtained from $R_{1\rho}$ were consistent with that obtained from the R_1 data for all four protonated ω-amino acids. However, the activation energies for amino group rotations obtained from $R_{1\rho}$ were all smaller than those obtained from R_1. This implies that, apart from classical interproton dipole−dipole interactions, some other interactions also affect the amino group rotations even though the exact nature for such effects remains unknown for the time being. Nevertheless, the temperature-dependent intermolecular interactions such as hydrogen bonding may be implicated, since the relaxation maximum appeared at different temperatures for $R_{1\rho}$ (220−300 K) and R_1 (350−450 K) where the strengths of hydrogen bonds were fairly different. Such temperature-

Table 3. Hydrogen Bond Lengths and Angles in the Crystal Structures of Glycine, 3-Aminopropanoic Acid (3-AP), 4-Aminobutyric Acid (4-AB), 5-Aminovaleric Acid (5-AVA), and 6-Aminocaproic Acid (6-ACA)

compounds	H-bond lengths (Å)			mean value (Å)	H-bond angles (N−H−O) (deg)		
3-AP[a]	2.795	2.753	2.833	2.794	159.4	163.8	173.9
4-AB[b]	2.733	2.751	2.767	2.750	172.4	168.8	168.1
5-AVA[c]	2.77	2.86	2.89	2.84			
6-ACA[d]	2.728	2.753	2.814	2.765	166	174	179
Glycine[e]	2.770	2.855	3.075	2.900	169.3	168.5	154.0

[a]Data taken from ref 18. [b]Data taken from ref 19. [c]Data taken from ref 20. [d]Data taken from ref 21. [e]Data taken from ref 59.

dx.doi.org/10.1021/jp211623n | J. Phys. Chem. B 2012, 116, 2096−2103

dependent interactions were probably also related to the fairly different τ_0 and C values obtained from the $R_{1\rho}$ and R_1 data (Table 2).

Figure 5a shows the plot of the rotational activation energy E_a for the amino groups as a function of the average length of

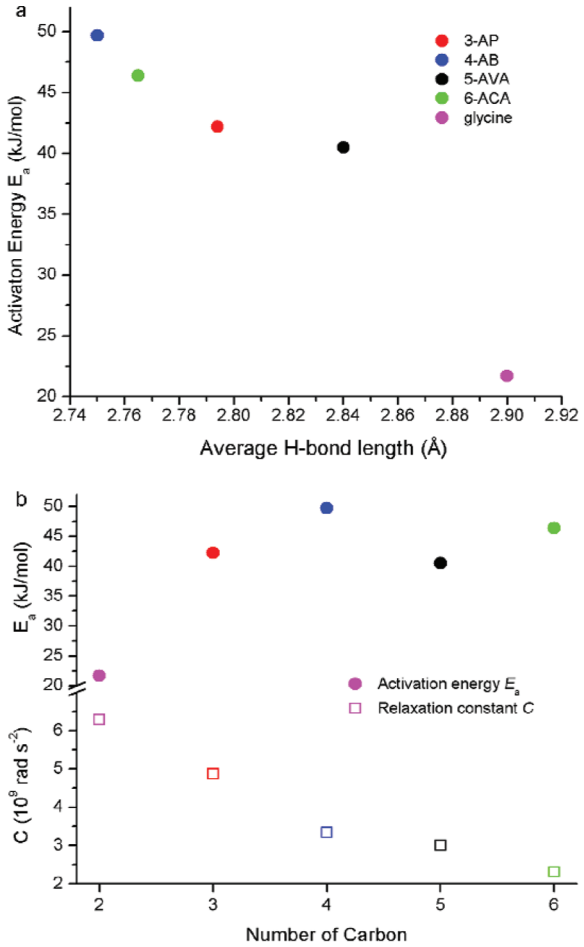

Figure 5. Motional parameters as a function of structural properties for glycine, 3-aminopropanoic acid (3-AP), 4-aminobutyric acid (4-AB), 5-aminovaleric acid (5-AVA), and 6-aminocaproic acid (6-ACA): (a) the plot of activation energy E_a for amino group rotation as a function of the average hydrogen-bond length; (b) E_a (filled symbols) and relaxation constant C (empty symbols) as a function of the carbon numbers in the molecules.

hydrogen bonds (Table 3) in which these amino groups are involved. It is apparent that the activation energy is inversely correlated with the length of hydrogen bonds and thus positively correlated with the hydrogen-bond strength. This indicates that the energy required for rotations of amino groups is used to overcome not only the interproton dipole−dipole interactions within the same molecule but also constrains from the intermolecular hydrogen-bonding network, in which these amino groups participate. Similar correlations have been found for D-, L-, and DL-aspartic acid[56] and α and β polymorphisms of L-glutamic acid.[57] A positive correlation was also observable for the activation energies of amino groups and the carbon-chain length in these molecules (Figure 5b). Interestingly, the activation energies for backbone motions were inversely correlated with the carbon-chain lengths of their backbones (Table 2), implying enhanced backbone flexibility with increased chain length. However, the relaxation constant C values for amino groups showed an inverse correlation with the carbon numbers in these molecules (Figure 5b). This is not surprising, since the increase of backbone chain length inevitably results in the increase of proton number and thus relaxation load.

CONCLUSIONS

This study showed that the molecular dynamics of ω-amino acids, namely, 3-AP, 4-AB, 5-AVA, and 6-ACA, had some structural dependence in the solid state. Proton relaxation processes were dominated by the 3-fold reorientations of amino groups for all of these ω-amino acids. A weak relaxation process was also present for 4-AB, 5-AVA, and 6-ACA probably related to their backbone motions, and such motions were much more pronounced for 5-AVA. With exceedingly long proton T_1 at 300 MHz, more motional details cannot be accessed easily with complex NMR methods such as DIPSHIFT or ^{13}C relaxation time measurements. The activation energies for amino group motions showed a positive correlation with the strength of hydrogen bonds involving amino groups in the crystals and the carbon-chain lengths, whereas such energies for the backbone motions were inversely correlated with the carbon-chain lengths.

ASSOCIATED CONTENT

Supporting Information

Figures showing ^{13}C CPMAS spectra and the signal intensity as a function of relaxation decay in ^1H T_1 measurements. This material is available free of charge via the Internet at http://pubs.acs.org.

AUTHOR INFORMATION

Notes

The authors declare no competing financial interest.

ACKNOWLEDGMENTS

The authors acknowledge financial support from National Basic Research Program of China (2010CB912501) and National Natural Science Foundation of China (20825520, 20903115, and 20921004). Jiming An at Center for Materials Research & Analysis of Wuhan University of Technology performed the DSC measurements as a paid service. Drs. Pingping Ren and Lei Chen are also thanked for their assistance in variable temperature NMR experiments.

REFERENCES

(1) Tang, H. R.; Covington, A. D.; Hancock, R. A. *Biopolymers* **2003**, *70* (3), 403.
(2) Lu, Z. B.; Nie, G. J.; Belton, P. S.; Tang, H. R.; Zhao, B. L. *Neurochem. Int.* **2006**, *48* (4), 263.
(3) Boutonnet-Fagegaltier, N.; Menegotto, J.; Lamure, A.; Duplaa, H.; Caron, A.; Lacabanne, C.; Bauer, M. *J. Pharm. Sci.* **2002**, *91* (6), 1548.
(4) Geppi, M.; Mollica, G.; Borsacchi, S.; Veracini, C. A. *Appl. Spectrosc. Rev.* **2008**, *43* (3), 202.
(5) Ren, P. P.; Reichert, D.; He, Q. H.; Zhang, L. M.; Tang, H. R. *J. Phys. Chem. B* **2011**, *115*, 2814.
(6) Ganapathy, S.; McDowell, C. A.; Raghunathan, P. *J. Magn. Reson.* **1982**, *50*, 197.
(7) Huang, J.; Jiang, L. M.; Ren, P. P.; Zhang, L. M.; Tang, H. R. *J. Phys. Chem. B* **2012**, *116*, 136.
(8) Weinstock, H. H.; Mitchell, H. K.; Pratt, E. F.; Williams, R. J. *J. Am. Chem. Soc.* **1939**, *61*, 1421.

(9) Derave, W.; Everaert, I.; Beeckman, S.; Baguet, A. *Sports Med.* **2010**, *40* (3), 247.
(10) Derave, W.; Oezdemir, M. S.; Harris, R. C.; Pottier, A.; Reyngoudt, H.; Koppo, K.; Wise, J. A.; Achten, E. *J. Appl. Physiol.* **2007**, *103* (5), 1736.
(11) Hill, C. A.; Harris, R. C.; Kim, H. J.; Harris, B. D.; Sale, C.; Boobis, L. H.; Kim, C. K.; Wise, J. A. *Amino Acids* **2007**, *32* (2), 225.
(12) Owens, D. F.; Kriegstein, A. R. *Nat. Rev. Neurosci.* **2002**, *3* (9), 715.
(13) Tillakaratne, N. J. K.; Medinakauwe, L.; Gibson, K. M. *Comp. Biochem. Physiol., Part A* **1995**, *112* (2), 247.
(14) Syrjanen, S. M.; Alakuijala, L.; Alakuijala, P.; Markkanen, S. O.; Markkanen, H. *Arch. Oral Biol.* **1990**, *35* (3), 189.
(15) Fergusson, D. A.; Hebert, P. C.; Mazer, C. D.; Fremes, S.; MacAdams, C.; Murkin, J. M.; Teoh, K.; Duke, P. C.; Arellano, R.; Blajchman, M. A.; Bussieres, J. S.; Cote, D.; Karski, J.; Martineau, R.; Robblee, J. A.; Rodger, M.; Wells, G.; Clinch, J.; Pretorius, R.; Investigators, B. *N. Engl. J. Med.* **2008**, *358* (22), 2319.
(16) Zhang, W. P.; Shao, J. M. *J. Biomed. Mater. Res., Part A* **2010**, *94A* (2), 450.
(17) Zhang, W. P.; Huang, Y. Q. *J. Polym. Environ.* **2011**, *19* (1), 177.
(18) Papavinasam, E.; Natarajan, S.; Shivaprakash, N. C. *Int. J. Pept. Protein Res.* **1986**, *28* (5), 525.
(19) Steward, E. G.; Player, R. B.; Warner, D. *Acta Crystallogr., Sect. B* **1973**, *29*, 2038.
(20) Honda, K.; Goto, M.; Kurahashi, M. *Chem. Lett.* **1990**, *1*, 13.
(21) Bodor, G.; Bednowit, A. L.; Post, B. *Acta Crystallogr.* **1967**, *23*, 482.
(22) Wang, Y. L.; Belton, P. S.; Tang, H. R. *Solid State Nucl. Magn. Reson.* **1999**, *14* (1), 19.
(23) Wang, Y. L.; Belton, P. S.; Tang, H. R.; Wellner, N.; Davies, S. C.; Hughes, D. L. *J. Chem. Soc., Perkin Trans. 2* **1997**, 899.
(24) Tang, H. R.; Belton, P. S.; Davies, S. C.; Hughes, D. L. *Carbohydr. Res.* **2001**, *330* (3), 391.
(25) Tang, H. R.; Belton, P. S. *Solid State Nucl. Magn. Reson.* **1998**, *12* (1), 21.
(26) Hills, B. P.; Wang, Y. L.; Tang, H. R. *Mol. Phys.* **2001**, *99* (19), 1679.
(27) Hills, B. P.; Tang, H. R.; Belton, P. S.; Khaliq, A.; Harris, R. K. *J. Mol. Liq.* **1998**, *75* (1), 45.
(28) Cai, W. Z.; Schmidt-Rohr, K.; Egger, N.; Gerharz, B.; Spiess, H. W. *Polymer* **1993**, *34* (2), 267.
(29) Zhang, L. M.; Tang, H. R.; Hou, G. J.; Shen, Y. D.; Deng, F. *Polymer* **2007**, *48* (10), 2928.
(30) Miyoshi, T.; Takegoshi, K.; Hikichi, K. *Polymer* **1997**, *38* (10), 2315.
(31) Tang, H. R.; Belton, P. S.; Ng, A.; Ryden, P. *J. Agric. Food Chem.* **1999**, *47* (2), 510.
(32) Tang, H. R.; Wang, Y. L.; Belton, P. S. *Solid State Nucl. Magn. Reson.* **2000**, *15* (4), 239.
(33) Tang, H. R.; Hills, B. P. *Biomacromolecules* **2003**, *4* (5), 1269.
(34) Taylor, R. E. *Concepts Magn. Reson., Part A* **2004**, *22A* (2), 79.
(35) Look, D. C.; Lowe, I. J. *J. Chem. Phys.* **1966**, *44* (8), 2995.
(36) Powles, J. G.; Mansfield, P. *Phys. Lett.* **1962**, *2* (2), 58.
(37) Powles, J. G.; Strange, J. H. *Proc. Phys. Soc.* **1963**, *82* (525), 6.
(38) Abragam, A. *The Principles of Nuclear Magnetism*; Oxford University Press: New York, 1961.
(39) Wang, Y. L.; Tang, H. R.; Belton, P. S. *J. Phys. Chem. B* **2002**, *106* (49), 12834.
(40) Zumbulyadis, N.; Henrichs, P. M.; Young, R. H. *J. Chem. Phys.* **1981**, *75* (4), 1603.
(41) Eichele, K.; Lumsden, M. D.; Wasylishen, R. E. *J. Phys. Chem.* **1993**, *97* (35), 8909.
(42) Hexem, J. G.; Frey, M. H.; Opella, S. J. *J. Am. Chem. Soc.* **1981**, *103* (1), 224.
(43) Kubo, R.; Tomita, K. *J. Phys. Soc. Jpn.* **1954**, *9* (6), 888.
(44) Wang, Y. L.; Belton, P. S.; Tang, H. R. *Chem. Phys. Lett.* **1997**, *268* (5−6), 387.
(45) Tang, H. R.; Wang, Y. L.; Belton, P. S. *Phys. Chem. Chem. Phys.* **2004**, *6* (13), 3694.
(46) Andrew, E. R.; Bryant, D. J.; Cashell, E. M.; Meng, Q. A. *FEBS Lett.* **1981**, *126* (2), 208.
(47) Andrew, E. R.; Hinshaw, W. S.; Hutchins, M. G.; Sjöblom, R. O. I.; Canepa, P. C. *Mol. Phys.* **1976**, *32* (3), 795.
(48) Krushelnitsky, A.; Zinkevich, T.; Mukhametshina, N.; Tarasova, N.; Gogolev, Y.; Gnezdilov, O.; Fedotov, V.; Belton, P.; Reichert, D. *J. Phys. Chem. B* **2009**, *113* (29), 10022.
(49) Andrew, E. R.; Hinshaw, W. S.; Hutchins, M. G.; Sjöblom, R. O. I. *Mol. Phys.* **1976**, *31* (5), 1479.
(50) Andrew, E. R.; Hinshaw, W. S.; Hutchins, M. G.; Sjöblom, R. O. I. *Mol. Phys.* **1977**, *34* (6), 1695.
(51) Lehmann, M. S.; Koetzle, T. F.; Hamilton, W. C. *J. Am. Chem. Soc.* **1972**, *94* (8), 2657.
(52) Koetzle, T. F.; Golic, L.; Lehmann, M. S.; Verbist, J. J.; Hamilton, W. C. *J. Chem. Phys.* **1974**, *60* (12), 4690.
(53) Alkaraghouli, A. R.; Cole, F. E.; Lehmann, M. S.; Miskell, C. F.; Verbist, J. J.; Koetzle, T. F. *J. Chem. Phys.* **1975**, *63* (4), 1360.
(54) Frey, M. N.; Koetzle, T. F.; Lehmann, M. S.; Hamilton, W. C. *J. Chem. Phys.* **1973**, *58* (6), 2547.
(55) McCall, D. W.; Douglass, D. C. *Appl. Phys. Lett.* **1965**, *7* (1), 12.
(56) Gu, Z. T.; Ebisawa, K.; McDermott, A. *Solid State Nucl. Magn. Reson.* **1996**, *7* (3), 161.
(57) Kitchin, S. J.; Ahn, S. B.; Harris, K. D. M. *J. Phys. Chem. A* **2002**, *106* (31), 7228.
(58) Taylor, R. E.; Dybowski, C. *J. Mol. Struct.* **2008**, *889* (1−3), 376.
(59) Jönsson, P. G.; Kvick, Å. *Acta Crystallogr., Sect. B* **1972**, *B 28* (6), 1827.